SECURITY CLASSIFICATION OF THIS PAGE (When Data Entered)

REPORT DOCUMENTATION PAGE

READ INSTRUCTIONS BEFORE COMPLETING FORM

1. REPORT NUMBER: 86-02	2. GOVT ACCESSION NO.
3. RECIPIENT'S CATALOG NUMBER	
4. TITLE (and Subtitle): Magnetomechanical Acoustic Emission - A Review	5. TYPE OF REPORT & PERIOD COVERED: Technical
6. PERFORMING ORG. REPORT NUMBER	
7. AUTHOR(s): Kanji Ono	8. CONTRACT OR GRANT NUMBER(s): N00014-81-K-0011
9. PERFORMING ORGANIZATION NAME AND ADDRESS: Materials Science and Engineering Department, 6532 Boelter Hall, University of California, Los Angeles, CA 90024	10. PROGRAM ELEMENT, PROJECT, TASK AREA & WORK UNIT NUMBERS: 61153N, RR011-08-01, NR 384-700
11. CONTROLLING OFFICE NAME AND ADDRESS: Physics Division Code 412, ONR-800 North Quincy Street, Arlington, Virginia 22217	12. REPORT DATE: September 1986
	13. NUMBER OF PAGES: 14
14. MONITORING AGENCY NAME & ADDRESS(if different from Controlling Office)	15. SECURITY CLASS. (of this report)
	15a. DECLASSIFICATION DOWNGRADING SCHEDULE

16. DISTRIBUTION STATEMENT (of this Report)

Unlimited

Reproduction in whole in part is permitted for any purpose of the U.S. Government

17. DISTRIBUTION STATEMENT (of the abstract entered in Block 20, if different from Report)

18. SUPPLEMENTARY NOTES

To be presented at the Eighth International Acoustic Emission Symposium and published in "Progress in Acoustic Emission III".

19. KEY WORDS (Continue on reverse side if necessary and identify by block number)

Iron, Nickel
Iron - Nickel Alloys
Acoustic Emission
Residual Stress
Magnetomechanical Acoustic Emission
Ferromagnetic Materials
Barkhausen noise

20. ABSTRACT (Continue on reverse side if necessary and identify by block number)

See Next Page

DD FORM 1 JAN 73 1473 EDITION OF 1 NOV 65 IS OBSOLETE

SECURITY CLASSIFICATION OF THIS PAGE (When Data Entered)

MAGNETOMECHANICAL ACOUSTIC EMISSION - A REVIEW

Kanji Ono
Department of Materials Science and Engineering
School of Engineering and Applied Science
University of California, Los Angeles, Calif. USA

Abstract

This article reviews magnetomechanical acoustic emission (MAE) that can be used in developing nondestructive testing techniques for residual stress measurements and microstructural characterization. Effects of metallurgical and magnetic parameters on MAE are considered drawing from basic studies on nickel and iron as well as from applied research on rail and wheel steels. Some of the observed features of MAE can be explained in terms of the domain theory. Practical applications require additional developmental efforts, but potential for useful residual stress analysis is well demonstrated.

1. Introduction

The motion of magnetic domain walls in ferromagnetic materials produces acoustic emission (AE). This type of AE was detected during magnetization of nickel [1], and during elastic loading of iron [2]. Applied stress dependence of this effect was found later [3-5]. Since this can become a nondestructive testing method for residual stress determination, we have conducted a series of experiments to determine its characteristics in various ferromagnetic materials [5-12]. The origin of observed AE is related to magnetostriction, so we call it magnetomechanical acoustic emission, abbreviated as MAE. It is also called magneto-acoustic emission [13], or acoustic Barkhausen effect [1].

When a ferromagnetic sample is placed in an alternating magnetic field, AE outputs are obtained at a regular interval as shown Fig. 1. This is a typical MAE signal. A typical experimental set-up is given in Fig. 2. An AE transducer, which should be insensitive to a magnetic field, was attached to a sample. A flux sensing coil and a Barkhausen noise (BN) probe are also employed. The output was fed to a preamplifier with a suitable bandpass filter, followed by an rms voltmeter for the signal intensity measurement and other devices for detailed waveform analysis. The intensity of MAE signals depends on a number of parameters [5-12]. These include magnetization scheme, the intensity and frequency of applied magnetic field, applied and residual stress, chemical composition, microstructure or heat treatment, prior cold working, test temperature and the frequency range of AE detection.

The observed effects due to these variables are complex and interrelated, but a certain combination of measured parameters appear to allow unique determination of residual stress or that of microstructure.

In this article, we review previous findings on MAE as well as the results of recent studies on MAE. Also described are the current understanding of basic mechanisms and suitable approaches for practical applications of MAE.

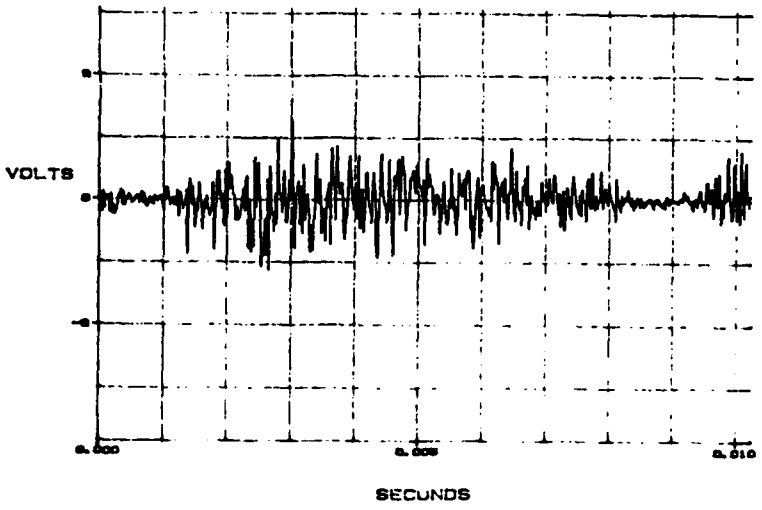

Fig. 1 MAE signal from a mild steel sample.

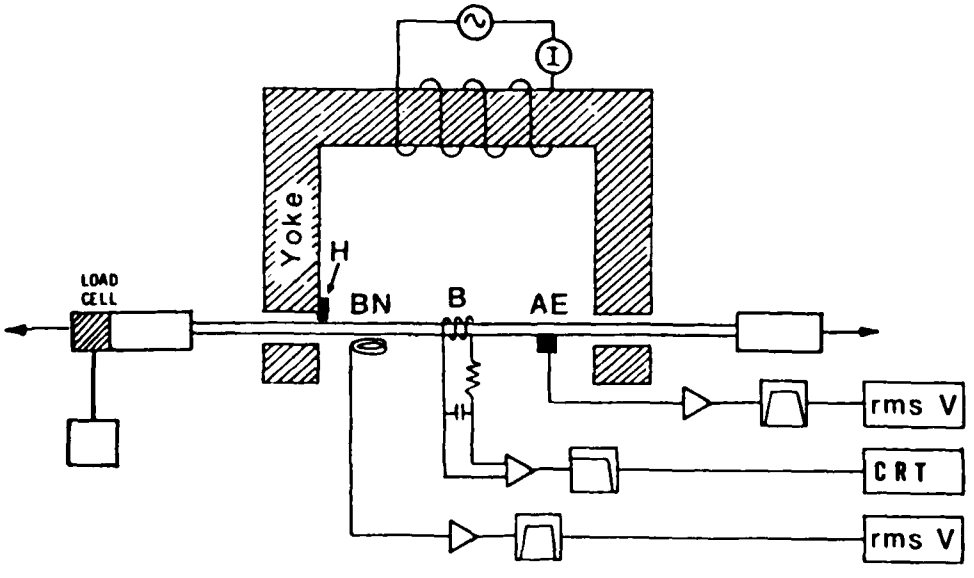

Fig. 2 Schematic diagram of experimental set up for MAE, BN and B responses.

2. Characteristics of MAE

2.1 Compositional effect

Typical changes of MAE output levels (nominally at 175 kHz) are shown against the applied field strength for seven ferromagnetic materials in Fig. 3 [6, 11]. No external stress was applied. Most samples were tested in either annealed or normalized condition. At low fields, nickel showed the highest MAE response and Fe-31%Ni alloy the lowest at any applied field strength. The very low response of the latter is due to its low magnetostriction behavior [10]. In intermediate Fe-Ni alloys, MAE intensity quickly saturates, then starts to increase again. Many materials exhibit similar two-stage behavior. These are referred to as Type I (at low fields) and Type II (at higher fields), respectively.

Effects of carbon content (up to 0.8%C) in iron-carbon alloys were examined. Increasing carbon content necessitated a higher value of magnetic field for detectable MAE. When a sufficiently strong magnetic field was applied, MAE intensity reached a maximum at 0.2%C [6].

Addition of Ni in Fe decreased the saturation level of Type I MAE. Starting at about 30%, MAE level increased with Ni additions, reaching the maximum in pure Ni. On the other hand, low Si addition in Fe increased Type I MAE, but 3 to 6.5% Si decreased the saturation level below Fe [11].

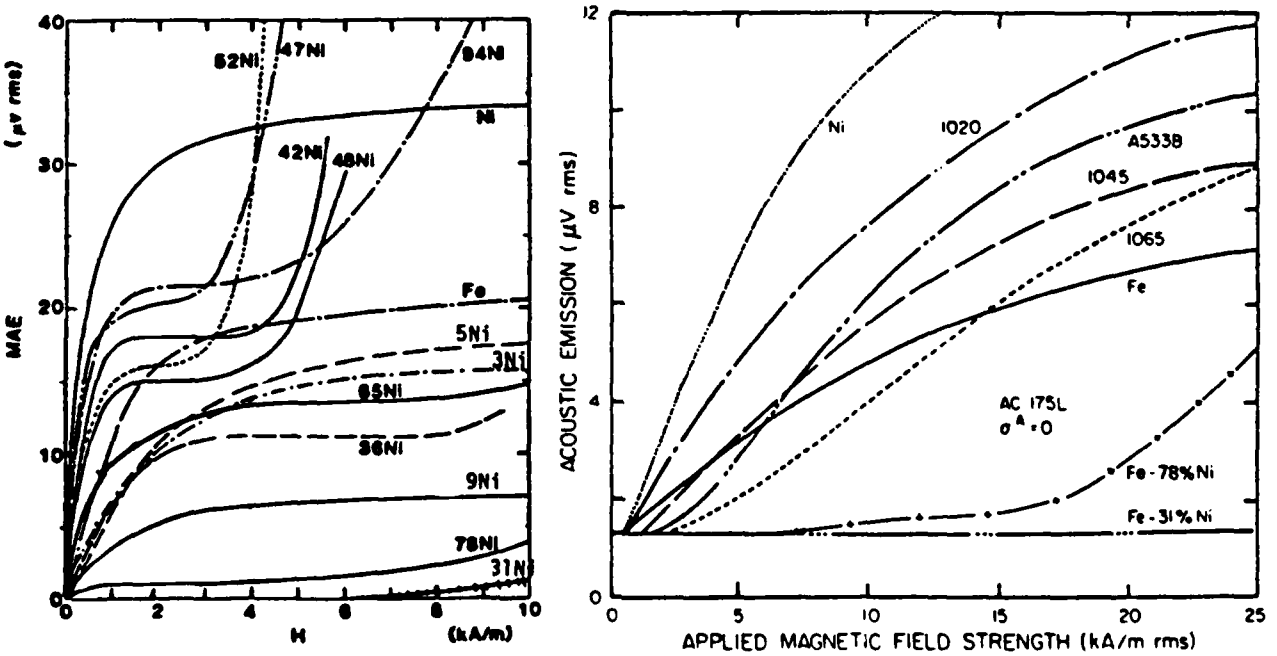

Fig. 3 AE vs. H for ferromagnetic materials.

2.2 Stress effect

The MAE intensity $\bar{V}_r$ (connected for background noise) vs. applied stress curves are shown in Fig. 4 [6]. Here, the results for A533B steel are given for a transducer having 500 kHz nominal center frequency at three levels of tensile strain (0, 1.4 and 15%). The AE intensity decreased by applying tensile or compressive stress. Most of the materials examined showed that, at constant applied magnetic field, MAE level became maximum at zero stress. However, in A533B steel and nickel, MAE increased slightly with the application of small compressive stress. Regardless of the stress directions, MAE level always decreased under a high stress. The effects of stress observed in laboratory size samples are exaggerated near zero stress. This arises from better transmission of acoustic energy through the grips. Thus, true stress dependencies can be revealed only when a very long sample is used with adequate damping materials on it. For this reason, MAE intensity alone cannot be used to determine the applied stress levels. This problem is unlikely to affect residual stress measurements, as no coupling effect is involved.

The ratio of the outputs of two transducers is a possible parameter to determine the stress state in a sample. Plots of AE ratio $R = \bar{V}_r(175\ kHz)/\bar{V}_r(500\ kHz)$ vs. stress in four materials are shown in Fig. 5. Here, $\bar{V}_r$ is the background corrected rms voltage and the nominal center frequencies are given in the parentheses. Iron and 1020 steel exhibited sharp decreases in R with stress, whereas steels with higher carbon contents had less variation in R with stress. The use of R can eliminate the uncertainty of transducer coupling, since a transducer can be designed with multiple resonances.

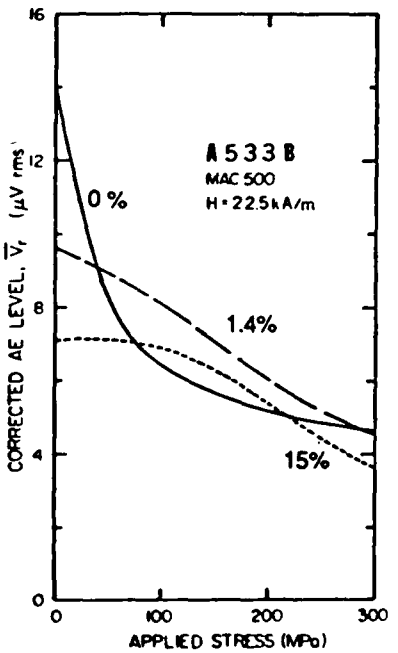

Fig. 4 $\bar{V}_r$ vs. applied stress for A533B steel deformed 0, 1.4, and 15%.

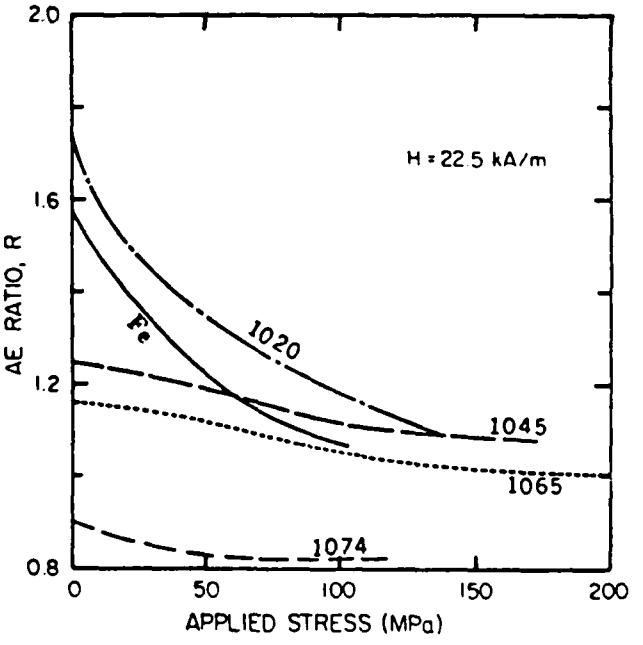

Fig. 5 AE ratio, R(175/550) vs. applied stress for iron and steels.

2.3 Microstructural effect

When the carbon content of iron-carbon alloys is varied, the fraction of ferrite or pearlite is changed. This, in turn, affects MAE behavior. When the carbon content is fixed, heat treatment alters the microstructure of a steel. When 1074 steel was oil-quenched, MAE output was severely depressed in comparison to the annealed condition [5-7]. Tempering of oil-quenched samples at 773 K restored MAE to about one-third the level of the annealed sample. Further tempering at 923 K increased the level to 70% of the annealed sample. These effects are clearly demonstrated in Fig. 6. A similar effect of heat treatment was observed in a number of steels. In a series of experiments [14], A533B steel samples were normalized, and tempered at 100 to 700 °C. Tempering up to 300 °C produced almost no change, but tempering at 600 or 650 °C increased MAE levels drastically (cf. Fig. 7). When A533B steel is normalized, bainitic structures are produced. Because of auto-tempering effects, microstructural changes are confined to dislocation recovery and carbide coarsening below 500 °C. Recrystallization of dislocated grains proceeds at 600 °C and tempering at 650 °C produces annealed ferrite plus carbide structures. Thus, MAE levels remain suppressed until tempering temperature reaches 600 °C.

In precipitation hardening steels, increased aging temperatures reduced the MAE level significantly. See Fig. 8 [15]. This effect is due to the pinning of domain boundaries by precipitate particles and can be used to uniquely identify heat treatment sequences even when the same hardness values are obtained as in maraging and PH-stainless steels. Similar effects of precipitate-domain wall interaction have also been reported in Fe- and Ni-base alloys [13].

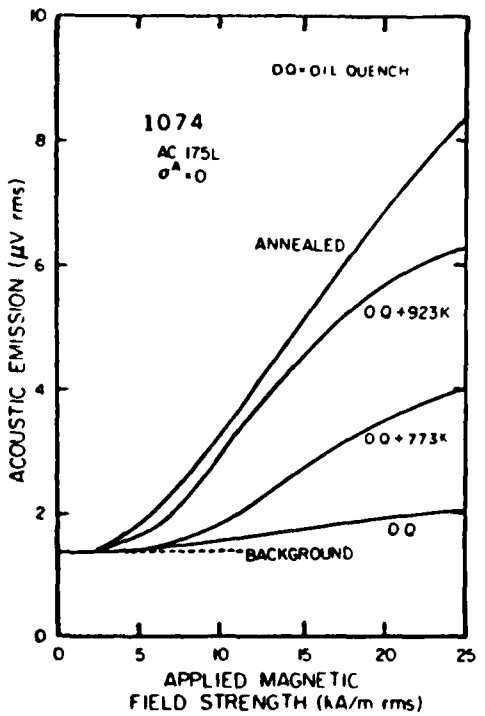

Fig. 6 AE vs. H for 1074 steel with different heat treatments.

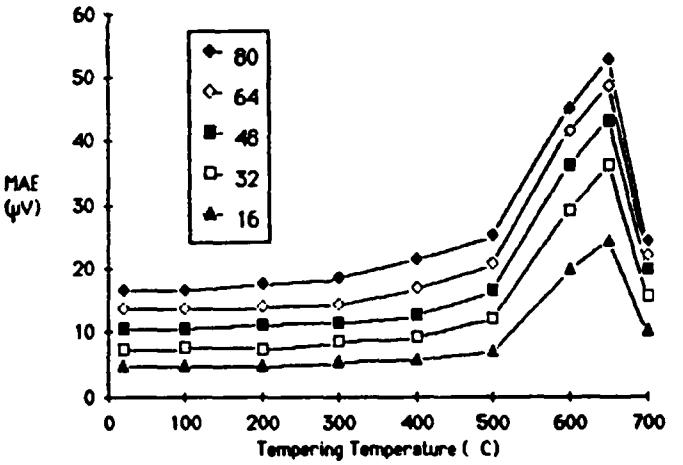

Fig. 7 MAE vs. tempering temperature of normalized A533B steel at five magnetization levels (marked in the insert).

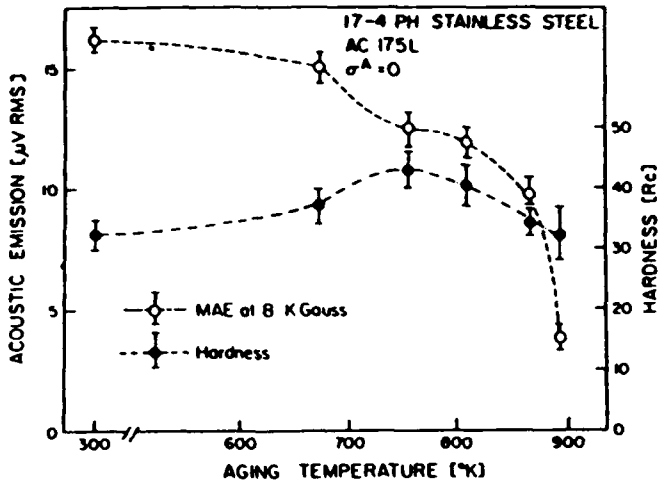

Fig. 8 MAE and hardness vs. aging temperature for 17-4 PH stainelss steel.

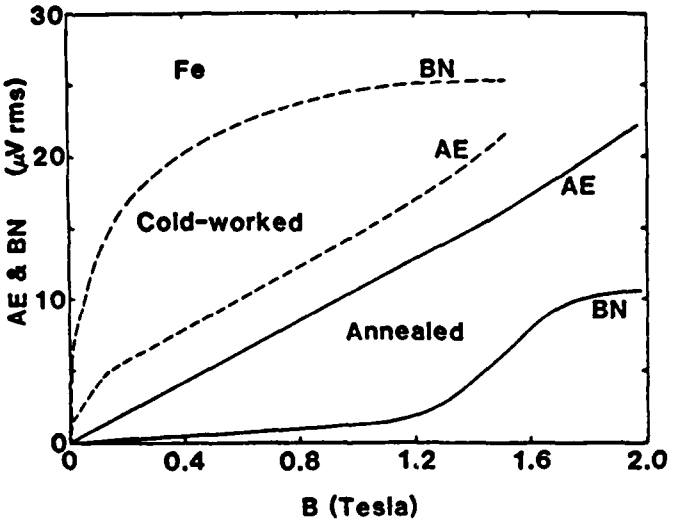

Fig. 9 MAE and BN vs. B for cold-worked and annealed iron with no applied stress.

2.4 Plastic deformation effect

Influence of prior cold work on MAE behavior was studied using Fe, Ni and steels [6, 9, 16]. The samples were progressively deformed in tension up to 18%. Typical variations are shown in Fig. 4. When the sample was deformed plastically, MAE decreased for a given field level and the shape of stress dependence curves also changed. However, this is partly due to changes in magnetization behavior caused by cold work. At a given magnetization level, MAE as well as Barkhausen noise (BN) increased as shown in Fig. 9 [9].

2.5 MAE and magnetic properties

MAE and BN responses of Fe, Ni and Fe-Ni alloys were evaluated together with the magnetic induction (see Fig. 9). In the annealed condition, MAE levels in iron and nickel increased linearly with B. On the other hand, BN responses were nonlinear. BN saturated before B reached its saturation level. This tendency became more obvious in cold-worked iron and nickel. MAE of cold-worked iron showed a linear dependence on B except at low B ($< 0.1B_s$). The linear slope in cold-worked iron was similar to that in annealed iron. On the other hand, MAE of cold-worked nickel behaved similarly to its BN response; both were parabolic and were quite different from the MAE vs. B curve of annealed nickel.

When a ferromagnetic sample is magnetized, its length changes. This is called magnetostriction. The relation between MAE and magnetostrictive strain, λ, in Ni (and three Fe-Ni alloys) is presented in Fig. 10, which shows three stages. The initial large increase of MAE at small λ corresponded to the steep portion of the B-H loop (Region I). Subsequently, MAE increase slowly (Regior II) until λ became close to its saturation value, λ_s. MAE increased further, even though λ saturated (Region III). This last region corresponds to Type II MAE behavior. λ_s in Ni was found to be -38×10^{-6}.

2.6 MAE waveforms

MAE and BN waveforms and signal envelopes during 60 Hz ac magnetization were recorded for a number of materials. The correlation between MAE and BN waveforms was made to establish the existence of high frequency signals during magnetization. BN responses were dependent on the type of detector and the domain structure of the material. Figure 11 shows the relationship between a 60 Hz sinusoidally varying magnetic field, magnetic induction, dB/dt and rectified MAE signal envelope for pure Fe at three field levels. B followed the sinusoidal variation of H at weak field (e.g, at H = 3.2 kA/m) and approached an approximate square wave at higher fields (H = 32-42 kA/m). The apparent phase lag between H and B is a consequence of hysteresis. At weak fields, duration of MAE signals was long and its peak value coincided with the maximum rate of magnetization. As field strength increased, the duration of the strongest part of the signal was reduced, but its intensity increased due to higher rates of magnetization. Again, the maximum MAE amplitude occurred at the maximum rate of flux change. The peak value of the MAE envelope continued to increase with field strength up to that required to attain magnetic saturation (as normally defined by measuring B_s via extrapolation). Further magnetic field increases did not change the peak amplitude of MAE observed at the peak of dB/dt. At high fields (H > 32 kA/m), B approaches a square wave with a peak amplitude of 2 Tesla. Duration of the MAE signal was short and a second peak in MAE started to emerge during the portion where dB/dt signals diminished.

3. Mechanisms

Barkhausen noise arises from a sudden motion of a magnetic domain wall, which is also a source of MAE [16]. It is well-known that B increases discontinuously in association with the jerky motion of domain walls. This is the case even when the applied magnetic field is increased slowly. A domain wall stops at a local energy minimum, then moving to a next minimum position abruptly. An MAE impulse is produced by the displacement resulting from differences in magnetostrictive strains in the two domains before and after the sudden movement (Region I in Fig. 10). The magnitude and direction can be described by an inelastic strain tensor $\Delta\varepsilon^*$ within the enlarged region of the domain, ΔV^*. Abrupt imposition of $\Delta\varepsilon^*$ generates stress waves, which are detected by an AE transducer as MAE. The peak output of a resonant AE transducer, V_p can be given by [7]

$$V_p = C\Delta\varepsilon^* \Delta V^*/\tau$$

where C is a constant and τ is the rise time of $\Delta\varepsilon^*$. The motion of 90° domain walls produces non-zero $\Delta\varepsilon^*$, but motion of 180° domain wall results in zero $\Delta\varepsilon^*$.

A finite inelastic strain is also expected when the local magnetization rotates away from the easy axis. The saturation magnetostriction of a single crystalline ferromagnetic material shows an anisotropy depending on the crystallographic direction. This rotation appears to proceed continuously, without sudden changes. Thus, while the rotation contributes to λ, but appears to produce little MAE as shown in Region II of Fig. 10 [10, 11].

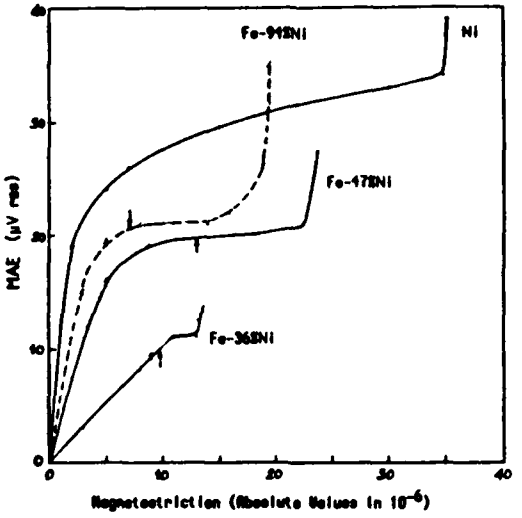

Fig. 10 MAE vs. λ for Ni and three Fe-Ni alloys.

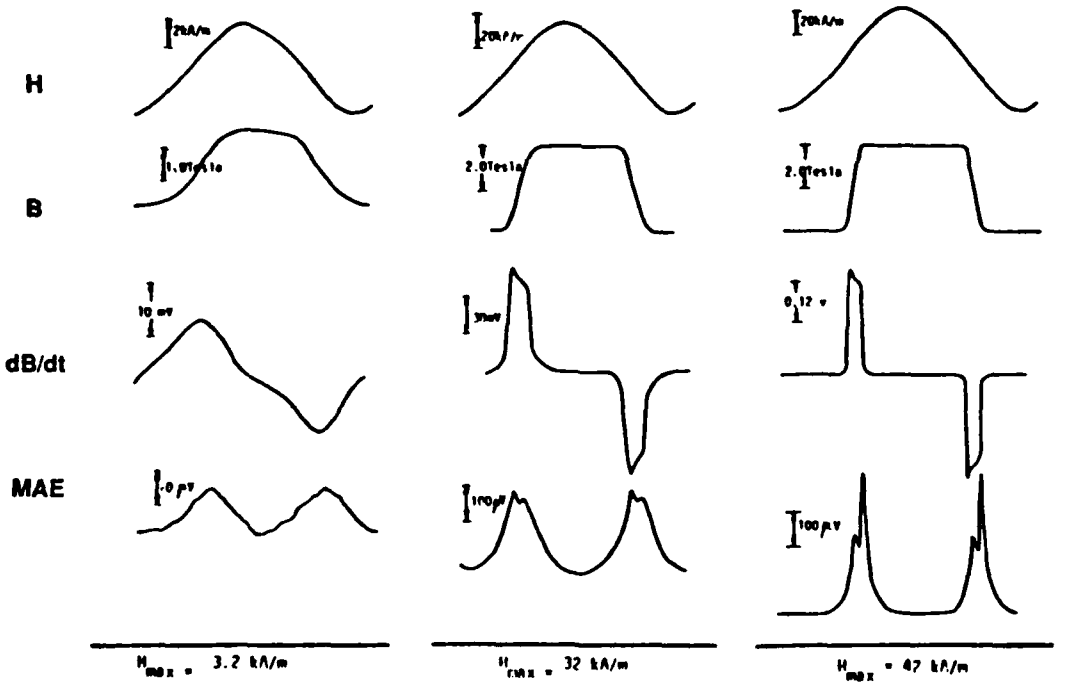

Fig. 11 H, B, dB/dt and MAE envelopes for iron at three field levels.

Under high magnetic fields, MAE increased without accompanying changes in magnetization and magnetostriction. This is shown in Region III of Fig. 10, where MAE increased despite little change in λ. This behavior appears to arise from sudden rotation or elimination of small magnetic domains, known as Neel spikes and closure domains [12].

A current understanding of MAE sources can be summarized as follow:

1. The motion of 180° domain wall does not contribute to MAE.
2. The 90° domain wall motion produces MAE through the abrupt generation of inelastic strain.
3. No significant MAE is produced during domain rotation.
4. MAE is proportional to the volume inside which the inelastic strain is produced.
5. MAE at high magnetization levels is accompanied by little changes in B and λ and is attributed to a sudden removal of small magnetic domains.
6. Stress reduces the size of magnetic domains. This decreases ΔV^* and consequently MAE intensity is reduced.

4. Applications

In field-inspections, an electromagnet, having either U- or E- shape yoke, is placed in proximity to the component surface for magnetization. One may also use a solenoid encircling the component. The penetration of magnetic intensity into the component will be limited by eddy current. When a yoke is utilized, the magnetic field distribution in the component having a large thickness becomes asymmetrical and non-uniform. However, this has not hampered MAE measurement. Mechanical stress conditions of structural components and weldments of mild steel and a pressure vessel steel were tested by MAE technique [8]. Stress dependent MAE responses were found (see Fig. 12).

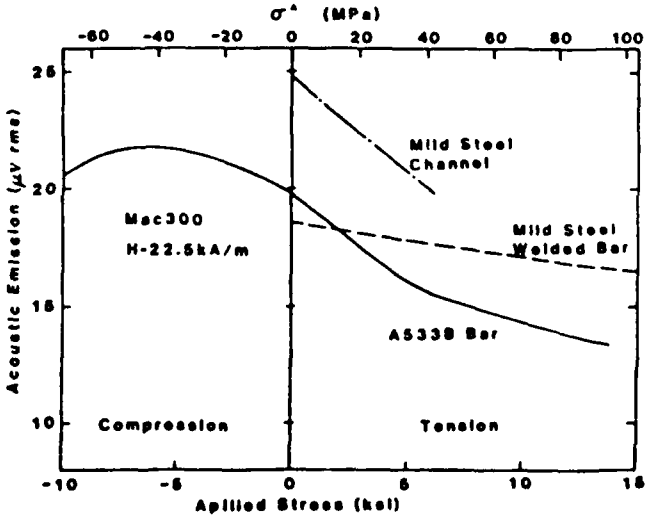

Fig. 12 MAE vs. stress for a mild steel channel, a welded mild steel and A533B steel bars.

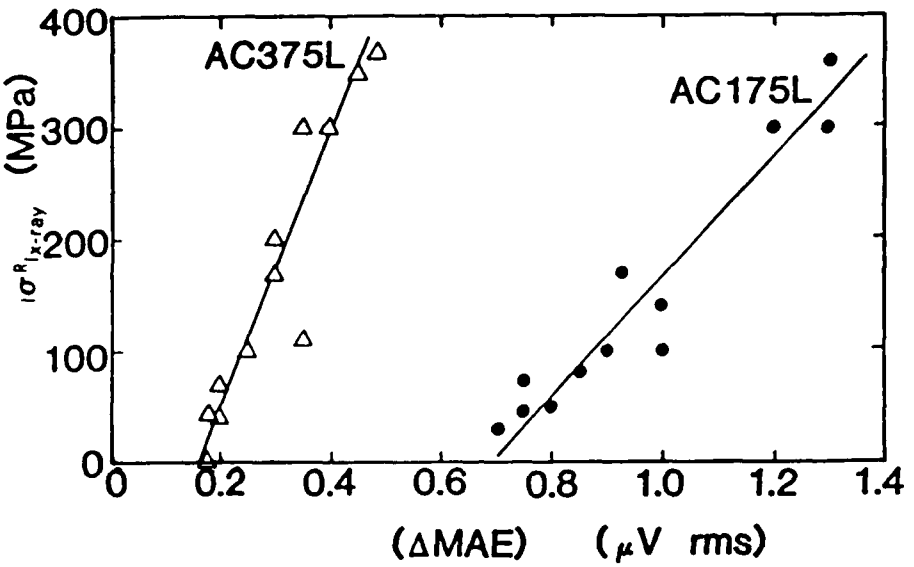

Fig. 13 Differences in MAE readings between reference and welded steel plates against stress measured by X-ray diffraction.

Another demonstration of MAE technique utilized a welded plate of mild steel. H-shaped slits were machined in a mild steel plate having 30 cm x 30 cm square shape with 0.95 cm thickness. The center slit was joined by manual arc welding and residual stresses were produced. For a comparison, the residual stresses were measured by X-ray diffraction. MAE responses and X-ray stresses at different positions in the center portion were measured and the results are given in Fig. 13. Here, MAE readings represent the differences between a reference plate and the welded plate. Although non-linear, the responses indicated measurable differences as a function of residual stress.

MAE technique has been applied to a laboratory testing of rail-force measurements [17]. The web-section of the rail was magnetized, and two different AE sensors were employed. Rail force up to 32 MPa in compression was applied over a temperature range of 26 to 82°C. It was found that R value analysis appears to provide the basis of rail force measurement. Figure 14 shows the results of this analysis. MAE was measured at 175 and 375 kHz, and AE ratios were calculated. The observed R values at 26 to 60°C decreased with increasing stress and were related to applied stress within a narrow scatter band. R values at 82°C were lower than this data range. Thus, by determining AE ratios, one can obtain the level of residual stress in a rail. When two completely different rails were tested, AE ratios still were within a reasonable range as shown in Fig. 15, allowing stress measurements within ± 8 MPa.

Practical techniques of MAE analysis can be developed in order to determine the stress state. A combination of MAE level and AE ratio, R, is a possible solution to indicate the stress state because of their different stress dependencies [6]. A unique correlation with stress was obtained using this approach in a mild steel channel and welded bar samples of A533B steel [8].

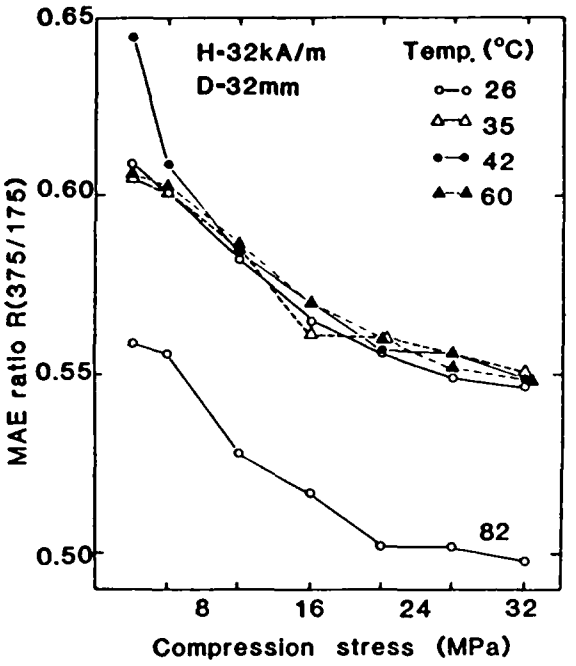

Fig. 14 Ratios of MAE signal levels at 375 kHz and 175 kHz against stress. Five different test temperatures were used with a fixed magnet-rail distance of 32 mm.

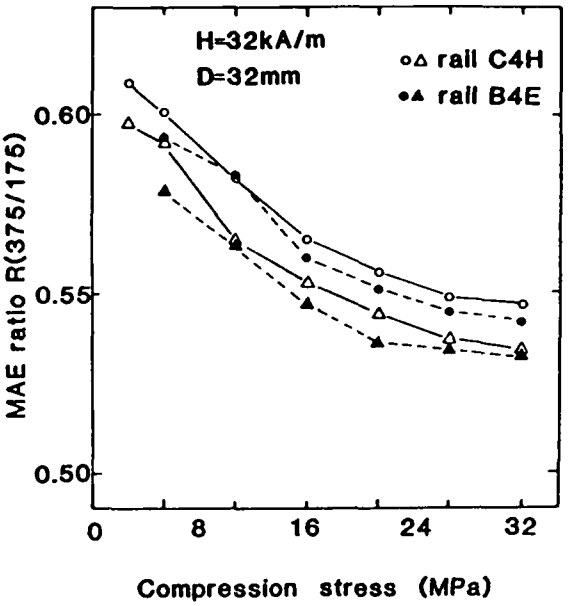

Fig. 15 Ratios of MAE signal levels at 375 kHz and 175 kHz against stress for two rails (results of two separate experiments shown). Fixed magnet-rail distance and magnetic field levels of 32 kA/m were used.

A different approach was developed using pattern recognition analysis assisted by a computer [18]. Here, envelopes of reference MAE waveforms (with different material and geometrical conditions and at various stress levels) are stored in a computer. For a typical magnetization frequency of 60 Hz, 16 to 32 data points per waveform will be adequate to describe a single waveform. When unknown MAE waveform is compared to the stored reference waveforms, a simple classification method based on the distance in a multidimensional vector space can classify the waveform to the nearest reference waveform. The stress state and material conditions are known for the reference, and MAE measurement of the unknown allows the determination of residual stress. Figure 16 shows an example of pattern classification using differently heat-treated samples BM, DM, EM and IM at four stress levels (N: 0 MPa, L: 11 MPa, M: 22 MPa and H: 33 MPa). Only three waveforms out of 64 were misclassified; i.e., a success rate of 95% was achieved.

	BML	BMM	BMH	BMN	DML	DMM	DMH	DMN	EML	EMM	EMH	EMN	IML	IMM	IMH	IMN
BML	4	0	0	0	0	0	0	0	0	0	0	0	0	0	0	0
BMM	0	4	0	0	0	0	0	0	0	0	0	0	0	0	0	0
BMH	0	0	4	0	0	0	0	0	0	0	0	0	0	0	0	0
BMN	0	0	0	4	0	0	0	0	0	0	0	0	0	0	0	0
DML	0	0	0	0	4	0	0	0	0	0	0	0	0	0	0	0
DMM	0	0	0	0	0	3	1	0	0	0	0	0	0	0	0	0
DMH	0	0	0	0	0	0	4	0	0	0	0	0	0	0	0	0
DMN	0	0	0	0	0	0	0	4	0	0	0	0	0	0	0	0
EML	0	0	0	0	0	0	0	0	4	0	0	0	0	0	0	0
EMM	0	0	0	0	0	0	0	0	0	4	0	0	0	0	0	0
EMH	0	0	0	0	0	0	0	0	0	1	3	0	0	0	0	0
EMN	0	0	0	0	0	0	0	0	0	0	0	4	0	0	0	0
IML	0	0	0	0	0	0	0	0	0	0	0	0	3	1	0	0
IMM	0	0	0	0	0	0	0	0	0	0	0	0	0	4	0	0
IMH	0	0	0	0	0	0	0	0	0	0	0	0	0	0	4	0
IMN	0	0	0	0	0	0	0	0	0	0	0	0	0	0	0	4

Fig. 16 Results of pattern classification via MAE envelopes under four different stress levels using four samples.

Acknowledgement

This research was supported by the Physics Program, Office of Naval Research.

References

1. A.E. Lord, Jr., *Acoustic Emission,* Vol. XI, W.P. Mason and R.N. Thurston (eds), Academic Press, New York, 1975, p. 290.

2. F.P. Higgins and S.H. Carpenter, "Sources of acoustic emission generated during the tensile deformation of pure iron," Acta Met. **26** (1978) 133.

3. H. Kusanagi, H. Kimura, and H. Sasaki, "Acoustic emission characteristics during magnetization of ferromagnetic materials," J. Appl. Phys. **50** (1979) 2985.

4. W.A. Theiner and E. Schneider, "Bestimmung von (Eigen-) Spannungen mit magetischen, magnetoelastischen und laufwegunabhangigen ultraschallverfahrfen," IZFP 790321-TW, June 1979.

5. M. Shibata and K. Ono, "Acoustic emission method for stress and strain determination," *Proc. of the Inst. of Acoustics Conference,* Chelsea College, London, England, April 1979.

6. K. Ono and M. Shibata, "Magnetomechanical AE of Iron and Steel," Mat. Eval. **38** (1980) 55.

7. K. Ono and M. Shibata, "Magnetomechanical AE for Residual Stress and Prior Strain Determination," *Advances in Acoustic Emission,* edited by H.L. Dunegan and W.F. Hartman, Dunhart, Knoxville, 1981, pp. 154-174.

8. K. Ono, M. Shibata and M. Man-Kwan, "Determination of Residual Stress by MAE," *Residual Stress for Designers and Metallurgists*, edited by L.J. Vande Walle, ASM, Metals Park, Ohio, 1981, pp. 223-243.

9. M. Shibata and K. Ono, "MAE - New Method for Nondestructive Stress Measurement," NDT International, 5 (1981) 227-234.

10. M. Man Kwan, K. Ono and M. Shibata, "Magnetomechanical Acoustic Emission - Temperature Effects", *Progress in Acoustic Emission, II, eds. M. Onoe et al*, Japan Soc. NDI, Tokyo, 1984, pp. 97-104.

11. M. Man Kwan, K. Ono and M. Shibata, "Magnetomechanical Acoustic Emission of Ferromagnetic Materials at Low Magnetization Levels (Type I Behavior)", J. Acoustic Emission, 3[3] (1984) 144-148.

12. M. Man Kwan, K. Ono and M. Shibata, "Magnetomechanical Acoustic Emission of Ferromagnetic Materials at High Magnetization Levels (Type II Behavior)", J. Acoustic Emission, 3[4] (1984) 90-203.

13. D.J. Buttle, C.B. Scruby, J.P. Jakubovics and G.A.D. Briggs, AERE - R11875, Harwell Lab., 1985.

14. K. Ono and O.Y. Kwon, unpublished. K. Ono, DoE Report for Contract No. ER80089, 1984.

15. I. Roman, S. Maharshak and G. Amir, "Magnetomechanical Acoustic Emission: A Non-destructive Characterization Technique of Precipitation Hardened Steels," J. Acoustic Emission, 2 (1983) 64.

16. M. Man Kwan, "Magnetomechanical Acoustic Emission of Ferromagnetic Materials," Ph. D. Thesis, Univ. of Calif., Los Angeles, 1983, pp. 1-418.

17. M. Shibata, E. Kobayashi and K. Ono, "The Detection of Longitudinal Rail Force via Magnetomechanical Acoustic Emission," J. Acoustic Emission, 4(4) (1985) 93-101.

18. M. Ohtsu and K. Ono, "Pattern Recognition Analysis of Magneto-Mechanical Acoustic Emission," J. Acoustic Emission, 3[2] (1984) 69-80.